Science Arts & Métiers (SAM)
is an open access repository that collects the work of Arts et Métiers Institute of Technology researchers and makes it freely available over the web where possible.

This is an author-deposited version published in: https://sam.ensam.eu
Handle ID: .http://hdl.handle.net/10985/9562

To cite this version :

Guillaume FROMENTIN, Benjamin DOEBBELER, Dieter LUNG - Computerized Simulation of Interference in Thread Milling of Non-Symmetric Thread Profiles - In: 15th CIRP Conference on Modelling of Machining Operations, Allemagne, 2015-06-11 - Procedia CIRP - 2015

Any correspondence concerning this service should be sent to the repository Administrator : scienceouverte@ensam.eu

Computerized Simulation of Interference in Thread Milling of Non-Symmetric Thread Profiles

Guillaume FROMENTIN[a,b*], Benjamin DÖBBELER[b], Dieter LUNG[b]

[a]*Arts et Metiers ParisTech Cluny, LaBoMaP, France*
[b]*Laboratory for Machine Tools and Production Engineering (WZL), RWTH Aachen University, Aachen, Germany*

* Corresponding author. Tel.: +33 385 595 330; fax: +33 385 595 370. *E-mail address:* guillaume.fromentin@ensam.eu

---

Abstract

Thread milling is a machining technique which is becoming widely used in specific contexts such as large diameter threading. Furthermore, compared to tapping, it is fully adapted to produce internal threads in difficult-to-cut materials, because the tool can be easily removed if a breakage occurs. For thread milling, as well as for form milling, groove and worm machining, geometrical considerations are critical aspects to succeed surface machining with the required accuracy. Interference phenomena may appear and appropriate cutter profiles and tool trajectories have to be defined to generate the desired shape. The proposed study is focusing on the threading of non-symmetric profile. A geometrical model computing the envelope profiles and using full parametrical definitions of the tool and thread is proposed. Its exploitation allows an analysis to explain and to quantify the influencing parameters on overcut. Then, an iterative method based on a direct approach, is proposed to define the tool design allowing to machine non-symmetric threads with good accuracy.

© 2015 The Authors. Published by Elsevier B.V. This is an open access article under the CC BY-NC-ND license
(http://creativecommons.org/licenses/by-nc-nd/4.0/).
Peer-review under responsibility of the International Scientific Committee of the “15th Conference on Modelling of Machining Operations

Keywords: Modelling; Milling; Thread, Interefence

---

1. Introduction

Thread milling allows producing both internal and external threads and is more and more used instead of tapping for high cost parts manufacturing. Thread milling induces a lower torque, a constant cutting speed, and the tool can be easily removed when breakage occurs. As a consequence, this technique is well adapted for low machinability materials.

Thread milling is a complex technique, due to the cutting tool geometry [1] and the milling trajectory. Thus, several studies focus on geometrical and mechanical aspects [2], cutting geometry effects [3, 4], penetration strategies [4, 5], cutting force modeling [6, 7] and dynamical stability [7].

Furthermore, there is a drawback linked to the thread milling technique, interferences appear and affect the thread accuracy. This geometrical phenomenon implies more, or less respectively, material is removed, i.e. overcut, undercut respectively. The reason is that the tool shape does not fit everywhere along its profile or for any tool position, with the desired surface which is intended to machine. This is quite common in machining with form tools, as in 5-axis flank milling [8-9], during helical groove [10-14], thread [15,16] and worm [17,18] grinding or milling with disc-type tools. From a global approach, interference can be compensated by adapting the tool profile, its trajectory, or both. Finally there are two main problems linked to the interference [10,17]. The first is to compute the geometrical error from the tool shape and its trajectory; it is named the direct problem. The second is to determine the tool profile from the desired surface geometry; it is named the inverse problem. Few studies are focused on the second approach [10,11,19], most of them only deal with the computation of geometrical errors [13,14,16,18], and someone may implement an iterative algorithm to the direct model to establish the tool profile for thread grinding [15] or for thread milling [20].

In internal thread milling, the configuration is different from groove, worm or thread machining with disc type tools, because the tool axis is parallel to the thread one, which is a less favorable situation from the interference point of view. Moreover, it is proven that the tool penetration can induce a significant overcut of the nominal thread, and the penetration has to respect different constraints to avoid it [5]. With symmetric thread profiles, the interference can be compensated during the full thread machining by changing the radius of the helical trajectory [20], which is not possible with non-symmetric thread profiles.

The present study deals with the interference compensation during the internal thread milling of non-symmetric thread profiles, such as buttress threads (S, GS & KS threads defined by DIN 513-1, DIN 55525, DIN 6063-1 standards). The used approach is based on a direct model of geometrical errors, and associated to an iterative algorithm for computing the tool profile correction and fitting the generated thread profile with the nominal one.

Nomenclature

Nominal thread characteristics:
α_i: i^{th} thread flank angle
D: major/nominal diameter (mm)
D_1: minor diameter (mm)
D_2: pitch diameter (mm)
L_c: crest length (mm)
L_g: groove length (mm)
P: pitch (mm)
$\mathbf{P_{ti}}$: i^{th} characteristic point of the nominal thread profile
R: major radius of the thread (mm)
R_1: minor radius of the thread (mm)
R_2: thread pitch radius (mm)
Mill cutter characteristics:
D_m: major diameter (mm)
D_{2m}: pitch diameter (mm)
L_{cfe}: length of the front cutting edge
$\mathbf{P_{mi}}$: i^{th} characteristic point of the mill profile
$\mathbf{P_{mi}^n}$: i^{th} characteristic point of the new mill profile
R_m: major radius of the thread (mm)
R_{1m}: minor radius of the thread (mm)
R_{2m}: thread pitch radius (mm)
Computed parameters:
E_r: radial error between nominal and generated thread (µm)
E_a: axial error between nominal and generated thread (µm)
R_{mc}: helix radius of the mill center trajectory (mm)
D_{mgt}: maximum diameter of the generated thread flank
Geometrical objects:
FTP(z): fundamental thread profile in (O,**E1**,**E3**) frame
MP(z_{ce}): mill profile in (O,**e1**,**e3**) frame
NTP(z): nominal thread profile in (O,**E1**,**E3**) frame
EMET(z_{ce}): envelope of the mill envelope trace in the (O,**E1**,**E3**) plane
GTP(z): generated thread profile in (O,**E1**,**E3**) frame

2. Thread milling parameterization

The parameterization of the thread milling operation is presented in Fig. 1. The nominal thread profile (**NTP**) is composed of 5 lines as shown in Fig. 2 and the mathematical formulation is the one used in [20]. Equations (1) give a full analytical definition of this profile and its 6 characteristic points in (O,$\mathbf{E_1}$,$\mathbf{E_3}$) reference system. They depend on the following parameters: thread radius (R, R_1, R_2), flanks angles (α_1, α_2) and groove and crest lengths (L_g, L_c) from which result the thread pitch (P).

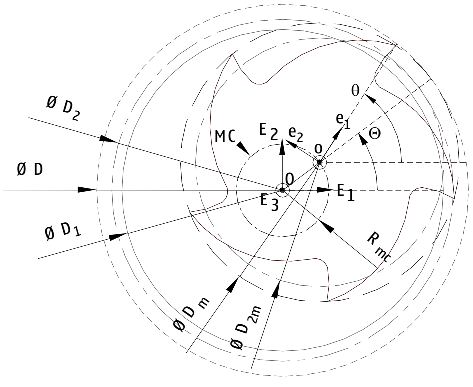

Fig. 1. Thread milling parameterization.

For the initial start of the simulation, the mill profile (**MP**) corresponds to the nominal thread one, i.e. same groove and crest lengths, same flank angles, but with considering lower diameters so the tool can enter into the hole.

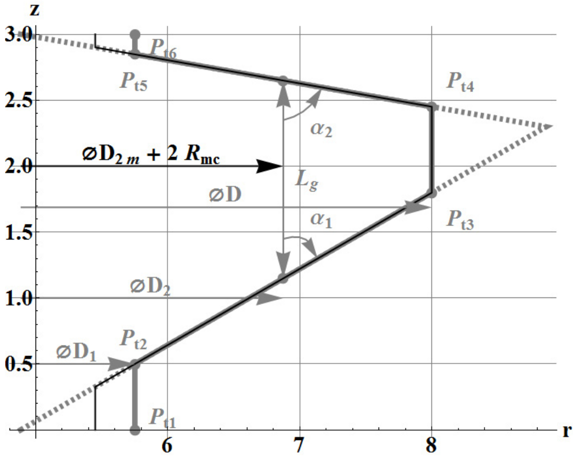

Fig. 2. Nominal thread profile (**NTP**) & mill profile (**MP**) in (O,$\mathbf{E_1}$,$\mathbf{E_3}$) – case B: D = 16 mm; P = 2.L_c = 2.L_g =3 mm; D_m = 10 mm; α_1 = 60°; α_2 = 80°).

$$\begin{aligned}
&\mathbf{NTP}(z) = [NTP_r(z), z]^T \\
&\mathbf{P}_{t1} = [P_{t1r}, P_{t1z}]^T = [R_1, 0]^T \\
&\mathbf{P}_{t2} = [P_{t2r}, P_{t2z}]^T = [R_1, (R_1 - R_2 + (L_c + (R_1 - \\
&\quad R_2)\,Cot[\alpha_1])\,Tan[\alpha_2]) / (Tan[\alpha_1] + Tan[\alpha_2])]^T \\
&\mathbf{P}_{t3} = [P_{t3r}, P_{t3z}]^T = [R, (R - R_2 + (L_c + (R - R_2) \\
&\quad Cot[\alpha_1])\,Tan[\alpha_2]) / (Tan[\alpha_1] + Tan[\alpha_2])]^T \\
&\mathbf{P}_{t4} = [P_{t4r}, P_{t4z}]^T = [R, L_g + (R_2 - R)\,Cot[\alpha_2] + \\
&\quad L_c\,Cos[\alpha_1]\,Sin[\alpha_2]\,Csc[\alpha_1 + \alpha_2]]^T \\
&\mathbf{P}_{t5} = [P_{t5r}, P_{t5z}]^T = [R_1, (R_2 - R_1 + (L_g + (R_2 - \\
&\quad R_1)\,Cot[\alpha_2])\,Tan[\alpha_1] + P\,Tan[\alpha_2]) / (Tan[\alpha_1] + \\
&\quad Tan[\alpha_2])]^T \\
&\mathbf{P}_{t6} = [P_{t6r}, P_{t6z}]^T = [R_1, P]^T \\
&P = L_c + L_g
\end{aligned} \tag{1}$$

In order to focus on well-defined thread applications, further down, the following relations (2) are considered, which match with buttress thread profile according to DIN 513-1 standard.

$$\begin{aligned} D_1 &= D - 1.5P \\ D_2 &= D - 0.75P \\ P &= 2L_c = 2L_g \end{aligned} \qquad (2)$$

3. Interference modelling

An interference model aims at the computation of geometrical errors. The steps of the algorithm are presented in Fig. 3. The used model is the one fully detailed in [20] and which is experimentally validated and confirmed by a different mathematical approach in [5]. The principle is as followed. The radius of the mill center trajectory (R_{mc}) is computed, as explained in Fig. 2. For each point of the mill profile, defined by its altitude z_{ce} in mill referential, the mill envelope trace (**MET**) in a thread cross section, i.e. (O, $\mathbf{E_1}$, $\mathbf{E_3}$) plane, is calculated. Then, the generated thread profile (**GTP**) is resulting from the envelope of every mill envelope traces (**EMET**). Finally the radial error (E_r) and the axial error (E_a) are obtained by calculating the distances from the **GTP** profile to the fundamental thread profile (**FTP**), as shown in equations (3) and Fig. 4.

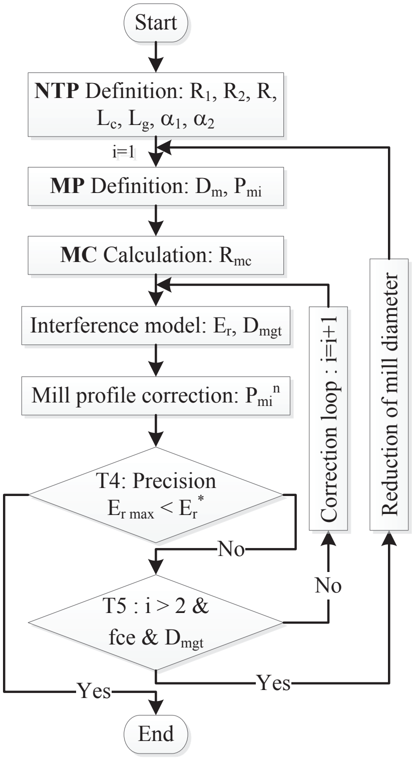

Start
NTP Definition: R_1, R_2, R, L_c, L_g, α_1, α_2
i=1
MP Definition: D_m, P_{mi}
MC Calculation: R_{mc}
Interference model: E_r, D_{mgt}
Mill profile correction: P_{mi}^n
T4: Precision $E_{r\,max} < E_r^*$
No
T5 : i > 2 & fce & D_{mgt}
No
Yes
Yes
End
Correction loop : i=i+1
Reduction of mill diameter

Fig. 3. Computerized simulation algorithm, included correction loops.

The Fig. 4 shows an example of a generated thread profile. Several points have to be underlined. The internal flank points of the **GTP** profile, at the D_1 diameter, are generated by **MP** profile points which are a completely different attitude is the tool referential, i.e. $\mathbf{P_{GTP5}}$ generated by $\mathbf{P_{m5g}}$. The extreme points of the mill profile, $\mathbf{P_{m3}}$ and $\mathbf{P_{m4}}$, generate a curved thread root, even if the mill profile is composed of lines. The errors and the root length depend greatly on the flank angles which are different for the upper and the lower flanks. Thus, the flank of the generated thread profile is much shorter that the **NTP** one and the maximum diameter of the generated thread (D_{mgt}) is calculated from equations (4).

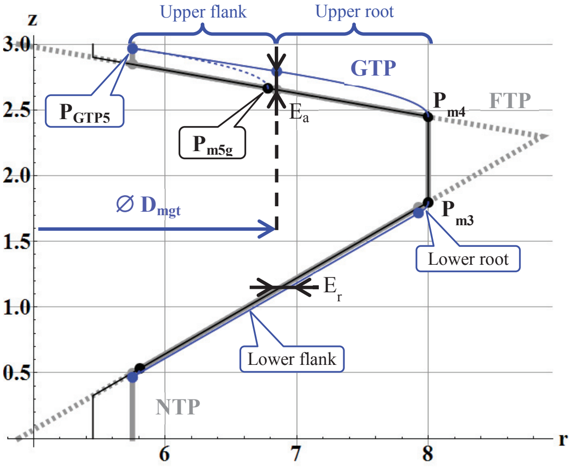

Fig. 4. Interference and errors – case B: D = 16 mm; P = 3 mm; D_m = 10 mm; α_1 = 60°; α_2 = 80°).

$$\begin{aligned} &E_r(z_{ce}) = \left\| \mathbf{EMET}(z_{ce}) - \mathbf{FTP}\left(\mathbf{EMET}(z_{ce}).\mathbf{E_3}\right) \right\| \\ &E_a(z_{ce}) = \left\| \mathbf{EMET}(z_{ce}) - \mathbf{FTP}(z_{ce}{*}) \right\| \\ &\mathbf{FTP}(z_{ce}{*}).\mathbf{E_1} = \mathbf{EMET}(z_{ce}).\mathbf{E_1} \end{aligned} \qquad (3)$$

$$\begin{aligned} &\mathbf{EMET}(P_{migz}).\mathbf{E_1} = R_1 \quad i \in (3,4) \\ &D_{mgt} = 2.\mathrm{Min}\left(\mathbf{EMET}(P_{m3z}).\mathbf{E_1}, \mathbf{EMET}(P_{m4z}).\mathbf{E_1}\right) \end{aligned} \qquad (4)$$

4. Parametric study

The overcut is resulting both from thread dimensions and tool ones. Table 1 is showing 8 configurations with constant flank angles and gives the maximal radial error ($E_{r\,max}$) for each flank. It has to be noticed that the error may vary from a 1000 factor, and up to 1 mm. Consequently, errors linked to interference have to be corrected to produce thread within a given tolerance.

The higher the P/D ratio is, the higher the radial error is. This ratio is in relation with the thread helix angle. From a geometrical point of view, when the thread helix angle is higher, the nominal thread surface crosses much more the tool envelope which has no helix angle, because it is a revolution surface. The error sensitivity to this ratio error is very high. Nevertheless, this parameter cannot be changed from the manufacturer position, and it is only linked to thread dimensions.

The higher the D_m/D ratio is, the higher the radial error is. Thus, it is constrained, because from a mechanical point of view a bigger mill diameter makes the tool stronger and limits

its deflection. Nonetheless, this ratio sensitivity on error is lower than the one of the previous ratio.

Table 1. Effect of thread and tool dimensions on radial error (α_1 = 60°; α_2 = 80°).

Case	D [mm]	P [mm]	D_m [mm]	P/D	D_m/D	$E_{r\,max}$ on lower fl. [µm]	$E_{r\,max}$ on upper fl. [µm]
A	16	1	10	0.06	0.63	8	85
B	16	3	10	0.19	0.63	72	797
C	32	1	10	0.03	0.31	1	12
D	32	3	10	0.09	0.31	10	104
E	32	6	10	0.19	0.31	39	409
F	32	1	20	0.03	0.63	4	42
G	32	3	20	0.09	0.63	36	386
H	32	6	20	0.19	0.63	143	1595

These observations are also established in [5,20]. Furthermore, the effect of the flank angle is studied, and Fig. 5 shows simulation results for α flank angles changing from 45° to 80°.

For a given flank angle, it is observed that the error on flank slightly increases, which means the generated flank has a different angle than the nominal one.

When the flank angle moves from 70° to 80°, the maximum radial error on the flank increases from 180 µm to 800 µm. Thus, the sensitivity to the flank angle is very high, but like with the P/D ratio, it is a fixed constraint. Moreover, it appears that the flank becomes shorter when the flank angle increases (as observed on Fig 4.). Consequently, in addition to the radial error, it is also needed to produce threads with a D_{mgt} diameter at least equal to the D nominal diameter to allow the assembly with the screws.

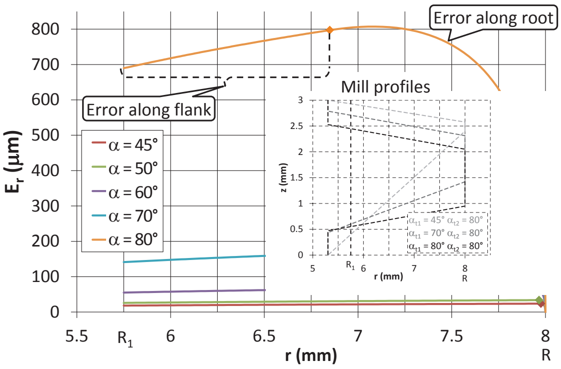

Fig. 5. Radial error along flanks and roots for different thread flank angles (case B: D = 16 mm; P = 3 mm; D_m = 10 mm).

5. Interference compensation

5.1. Simulation algorithm

The strategy for the interference compensation is mainly based on modification of the mill profile (**MP**). An iterative approach and the direct model for the error computation are used. Fig. 6 presents the correction algorithm which is integrated as a loop in the simulation detailed in Fig. 3. Fig. 7 shows the geometrical construction for the mill profile correction.

The main idea is to shift extreme points of the mill profile flanks prohibit the overcut, i.e. $\mathbf{P}_{m2}$ and $\mathbf{P}_{m3}$ for the lower flank, and $\mathbf{P}_{m4}$ and $\mathbf{P}_{m5}$ for the upper flank are modified. Nonetheless, there are constraints relatively to the thread geometry and several cases may appear.

First of all, the 1st test concerns the flank length. It is a condition expressed by equation (5), and the length of the front cutting edge (same condition than for the 3rd test). On the one hand, the flank has to be long enough, but on the other hand the front cutting edge length cannot be reduced over a too low value which makes the tool too brittle. At the simulation start, a low length of the front cutting edge (fce) may result directly from nominal thread geometry.

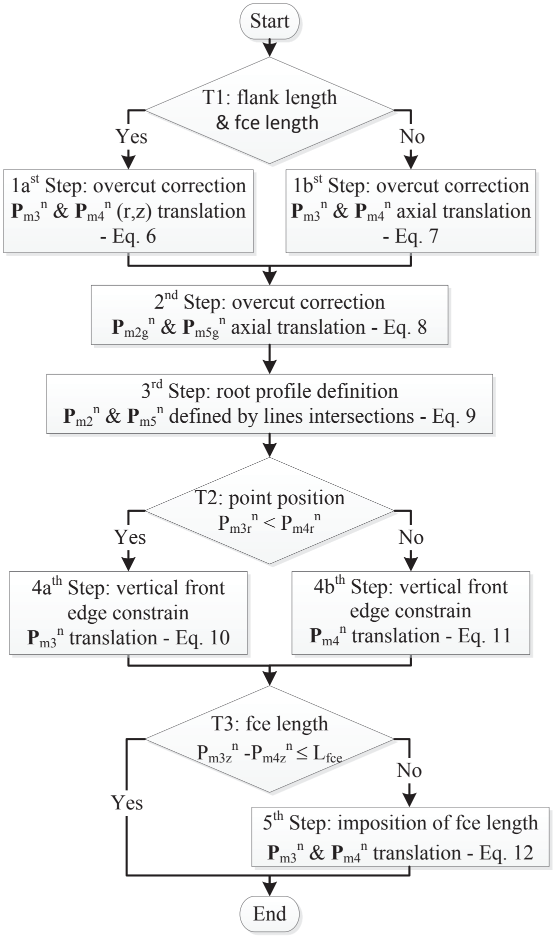
Start
T1: flank length & fce length
Yes
No
1ast Step: overcut correction $\mathbf{P}_{m3}^{\ n}$ & $\mathbf{P}_{m4}^{\ n}$ (r,z) translation - Eq. 6
1bst Step: overcut correction $\mathbf{P}_{m3}^{\ n}$ & $\mathbf{P}_{m4}^{\ n}$ axial translation - Eq. 7
2nd Step: overcut correction $\mathbf{P}_{m2g}^{\ n}$ & $\mathbf{P}_{m5g}^{\ n}$ axial translation - Eq. 8
3rd Step: root profile definition $\mathbf{P}_{m2}^{\ n}$ & $\mathbf{P}_{m5}^{\ n}$ defined by lines intersections - Eq. 9
T2: point position $P_{m3r}^{\ n} < P_{m4r}^{\ n}$
Yes
No
4ath Step: vertical front edge constrain $\mathbf{P}_{m3}^{\ n}$ translation - Eq. 10
4bth Step: vertical front edge constrain $\mathbf{P}_{m4}^{\ n}$ translation - Eq. 11
T3: fce length $P_{m3z}^{\ n} - P_{m4z}^{\ n} \le L_{fce}$
Yes
No
5th Step: imposition of fce length $\mathbf{P}_{m3}^{\ n}$ & $\mathbf{P}_{m4}^{\ n}$ translation - Eq. 12
End

Fig. 6. Correction algorithm of MP mill profile points.

During the 1st step, if it is necessary to increase the flank length and if it can be, $\mathbf{P}_{m3}$ and $\mathbf{P}_{m4}$ are translated in r & z directions as defined by equations (6). If not, it is most of the time after the 1st correction loop, when the **MP** height has been adjusted, these 2 points are only shifted in the axial direction from the axial error (equations (7)) in order to get the new points (noted with a "n" exponent).

$$D_{mgt} < D \qquad (5)$$

$$\begin{aligned}\mathbf{P}_{m3}{}^{n} &= \mathbf{P}_{m3} - (\mathbf{EMET}(P_{m3z}) - \mathbf{NTP}_{B}(P_{m3z})) \\ \mathbf{P}_{m4}{}^{n} &= \mathbf{P}_{m4} - (\mathbf{EMET}(P_{m4z}) - \mathbf{NTP}_{B}(P_{m4z}))\end{aligned} \tag{6}$$

$$\begin{aligned}\mathbf{P}_{m3}{}^{n} &= \mathbf{P}_{m3} + [0, E_a(P_{m3z})]^T \\ \mathbf{P}_{m4}{}^{n} &= \mathbf{P}_{m4} - [0, E_a(P_{m4z})]^T\end{aligned} \tag{7}$$

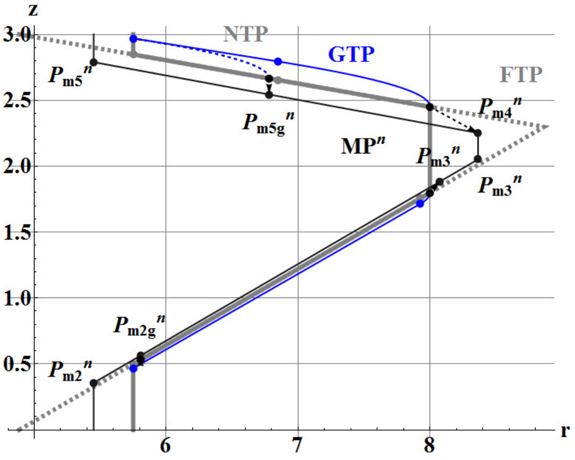

Fig. 7. Radial error along flanks during correction algorithm (case B: D = 16 mm; P = 3 mm; D_m = 10 mm; α_{t1} = 60°; α_{t2} = 80°).

The 2nd step consists of shifting the two mill profile points, $\mathbf{P}_{m2g}$ and $\mathbf{P}_{m5g}$, axially from the axial error, which generate the inner extreme points of the flanks. Equations (8) are applied.

$$\begin{aligned}\mathbf{P}_{m2g}{}^{n} &= \mathbf{P}_{m2g} + [0, E_a(P_{m2gz})]^T \\ \mathbf{P}_{m5g}{}^{n} &= \mathbf{P}_{m5g} - [0, E_a(P_{m5gz})]^T\end{aligned} \tag{8}$$

The 3rd step, the new points $\mathbf{P}_{m2}{}^{n}$ and $\mathbf{P}_{m5}{}^{n}$ are built by extension of flank lines, with considering the equations (9).

$$\begin{aligned}\mathbf{P}_{m2}{}^{n} &= (\mathbf{P}_{m2g}{}^{n}\mathbf{P}_{m3}{}^{n}) \cap (\mathbf{P}_{m1}\mathbf{P}_{m6}) \\ \mathbf{P}_{m5}{}^{n} &= (\mathbf{P}_{m5g}{}^{n}\mathbf{P}_{m4}{}^{n}) \cap (\mathbf{P}_{m1}\mathbf{P}_{m6})\end{aligned} \tag{9}$$

After the 1ast step, the $\mathbf{P}_{m3}{}^{n}$ and $\mathbf{P}_{m4}{}^{n}$ points are not vertically aligned because they were translated in the r & z directions with different vectors. Then, the 4th step shifts one of these two points to the right side. Depending on the 2nd test, Equation (10), (11) respectively, is used for the $\mathbf{P}_{m3}{}^{n}$ point, for the $\mathbf{P}_{m4}{}^{n}$ point respectively.

$$\mathbf{P}_{m3}{}^{n} = (\mathbf{P}_{m2}{}^{n}\mathbf{P}_{m3}{}^{n}) \cap (\mathbf{P}_{m4}{}^{n}, \mathbf{E}_3) \tag{10}$$

$$\mathbf{P}_{m4}{}^{n} = (\mathbf{P}_{m4}{}^{n}\mathbf{P}_{m5}{}^{n}) \cap (\mathbf{P}_{m3}{}^{n}, \mathbf{E}_3) \tag{11}$$

Moreover, the initial step may also translate the $\mathbf{P}_{m3}{}^{n}$ and $\mathbf{P}_{m4}{}^{n}$ points to the right side of the extreme right point of the fundamental thread profile (**FTP**). Practically, it means in this case that the $\mathbf{P}_{m3}{}^{n}$ point is up to the $\mathbf{P}_{m4}{}^{n}$ point, which is conditioned by the 3rd test. Then, if it is necessary, $\mathbf{P}_{m3}{}^{n}$ and $\mathbf{P}_{m4}{}^{n}$ points are one more time translated along the flanks with respecting equations (12), in order not to have a too short front cutting edge. It is necessary, but reduces the flank length.

$$\begin{aligned}(\mathbf{P}_{m4}{}^{n} - \mathbf{P}_{m3}{}^{n}).\mathbf{E}_1 &= 0 \\ (\mathbf{P}_{m4}{}^{n} - \mathbf{P}_{m3}{}^{n}).\mathbf{E}_3 &= L_{fce}\end{aligned} \tag{12}$$

The correction algorithm is completed after these 4 steps, and from the new mill profile (**MP**$^{\mathbf{n}}$), the error computation can be run again. As shown on Fig. 7, the corrected mill profile is thinner and deeper than the thread crest to machine initially. However, the generated thread profile will match the flanks of the nominal thread profile because of the overcut. The generated thread profile is effectively deeper than the nominal one, which does not make any problem; it is usually not standardized, e.g. for M metric thread.

The global simulation, presented Fig. 3, uses this correction loop until two conditions are realized. The 1st corresponds to the 4th test on the obtained precision vs the desired precisions ($E_r{}^*$). The 5th test is necessary to stop the correction loop after 2 iterations if the front cutting edge is equal to the minimum value, i.e. L_{fce}, and if the D_{mgt} diameter is still not large enough. If this case, it is clearly impossible to produce the thread with the tool having the input diameter. It may be possible will a smaller milling cutter, and then the D_m mill diameter has to be decreased. If it is still impossible with considering a smaller tool, then it has to be concluded that the desired thread profile cannot be obtained by thread milling. Thus, another threading technique like cut tapping, or form tapping for a greater precision [21], has to be chosen.

5.2. Applications of the computerized simulation

It is considered the thread milling case G, cf. Table 1. The initial maximum radial error is near 390 μm on the upper flank and 36 μm one the lower one. Fig. 8 presents the error along the flanks after each correction loop.

The maximal error after the 1st loop is drastically reduced to 6 μm. The upper flank reaches the R radius. Because α_2 flank angle is higher than the one on the lower flank, the error is more important on it. Thus, the correction algorithm translates further the $\mathbf{P}_{m4}$ point in r & z directions than the $\mathbf{P}_{m3}$ point (1ast step). The 4ath step shifts the $\mathbf{P}_{m3}$ point to the right side to align vertically these two points, then it results the lower flank length is longer than needed.

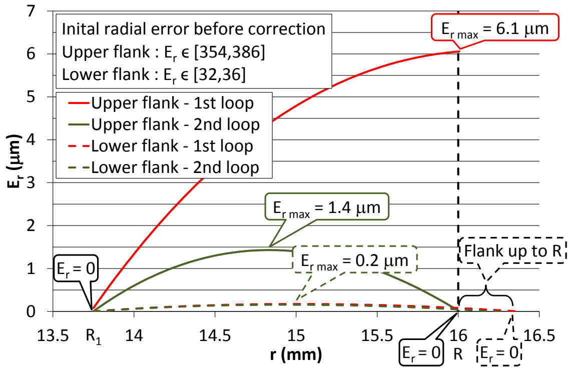

Fig. 8. Radial error along flanks during correction algorithm (case G: D = 32 mm; P = 3 mm; D_m = 20 mm; α_{t1} = 60°; α_{t2} = 80°).

During the 2nd correction loop, 1bth step is applied, the points are only vertically shifted, and the flank length is not affected. The resulting radial error becomes insignificant on both flanks. This error can be considered to be null on the flanks extreme points, which is the principle of the correction algorithm. Then, the goal is reached, additional loops are useless, and this case was solved with only two iterations.

Moreover, the error being null at the extreme flank points and having a parabolic form between these points, it can be deduced that the exact solution to fit the nominal thread profile along the entire flank, is not a straight line. Nevertheless, the error being already so small, and also other phenomena that cause interference appear (tool bending, machine error), it is really considered that the simulation is sufficient enough to improve the thread accuracy.

The case B is presented on Fig. 9. The initial and maximal radial error is around 800 µm on the upper flank. Here three correction loops are needed to obtain no error on the extreme upper flank points. The residual radial error reaches 9 µm. A better profile cannot be obtained with a mill profile composed of straight lines, however it is considered to be sufficient enough. Furthermore, the main point in this application is concerning the upper flank length which does not match the R nominal thread radius. The root length of the nominal thread is initially low vs the overcut to correct, and the algorithm enforces a minimum front cutting edge length which equals to L_{fce} = 0.2 mm. Then, in this case the new mill profile is modified by the 5th step of the algorithm at each loop. Consequently, the profile cannot be higher because of the fce length constraint, and then no more flank can be generated.

In this case, the mill diameter being already low, it might not be reduced anymore. Nonetheless, the accuracy may be sufficient; it depends on the required precision. Furthermore, it also has to be considered that the root is tangent to the flank and this curve smoothly evolves. Then, for a given interval tolerance, the flank which contributes effectivity to the assembly with the screw, may be partially the root of the generated thread.

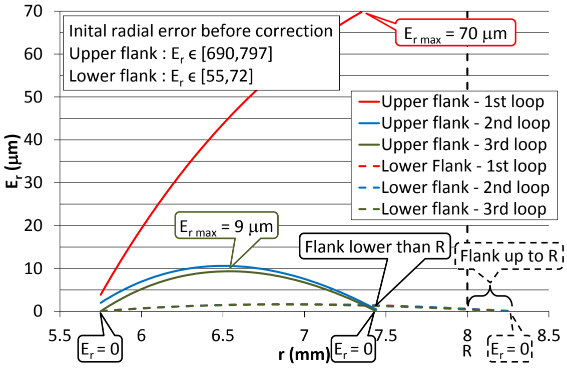

Fig. 9. Radial error along flanks during correction algorithm (case B: D = 16 mm; P = 3 mm; D_m = 10 mm; α_{t1} = 60°; α_{t2} = 80°).

6. Conclusion

This study presents an iterative algorithm for correcting the thread milling overcut by modifying the mill profile. This approach uses a direct model which has been already experimentally validated [20] and is fully adapted for non-symmetric thread profiles. The results are:

- a full analytical formulation of non-symmetric thread profiles,
- an algorithm, using a direct model of interference, and which shows high performance,
- and a global approach about the possibility to machine accurate threads with using thread milling, which would be experimentally validated with considering other aspects (tool bending…).

Furthermore, about the understanding of interference in thread milling, it is also established that the perfect solution for the mill flank profile, is not exactly a straight line, but it can be approximated very precisely by it.

The proposed simulation is only available for thread milling of profiles composed of straight lines. Further works would consider curved thread profiles, such as Rd round thread. Thus, the approach would consider the inverse problem, i.e. build the mill profile directly from the thread one, and not an iterative method.

References

[1] Fromentin G, Poulachon G. Geometrical analysis of thread milling – Part 1: Evaluation of tool angles. Int J Adv Manuf Tech 2010; 49(1):73-80.
[2] Fromentin G, Poulachon G. Geometrical analysis of thread milling - Part 2: Calculation of uncut chip thickness. Int J Adv Manuf Tech 2010; 49(1):81-87
[3] Araujo AC, Fromentin G, Poulachon G. Analytical and experimental investigations on thread milling forces in titanium alloy. Int J Mach Tool Manu 2013; 67:28-34.
[4] Sharma VS, Fromentin G, Poulachon G, Brendlen R. Investigation of tool geometry effect and penetration strategies on cutting forces during thread milling. Int J Adv Manuf Tech 2014; 74:963-972.
[5] Fromentin G, Sharma VS, Poulachon G, Paire Y, Brendlen R. Effect of thread milling penetration strategies on the dimensional accuracy. J Manuf Sci E-T ASME 2011; 133(4):1-13.
[6] Araujo AC, Silveira JL, Jun MBG, Kapoor SG, DeVor R. A model for thread milling cutting forces. Int J Mach Tool Manu 2006; 46:2057–2065.
[7] Wana M, Altintas Y. Mechanics and dynamics of thread milling process. Int J Mach Tool Manu 2014; 87:16-26.
[8] Redonnet JM, Rubio W, Dessein G. Side milling of ruled surfaces: Optimum positioning of the milling cutter and calculation of interference. Int J Adv Manuf Tech 1998; 14/7:459-465.
[9] Chaves-Jacob J, Poulachon G, Duc E. New approach to 5-axis flank milling of free-form surfaces: Computation of adapted tool shape. Comput Aided Design 2009; 41/12:918-929.
[10] Kang SK, Ehmann KF, Lin C. A CAD approach to helical groove machining Part 1: Mathematical model and model solution. Int J Mach Tool Manu 1996; 36(1):141-153.
[11] Hsieh JF. Mathematical model and sensitivity analysis for helical groove machining. Int J Mach Tool Manu 2006; 46(10):1087-1096.
[12] Sheth DS, Malkin S. CAD/CAM for geometry and process analysis of helical groove machining. CIRP Ann-Manuf Techn 1990; 39(1):29–132.
[13] Wu W, Li J, Feng Q. Simulation of the surface profile of the groove bottom enveloped by milling cutters in single screw compressors. Comput Aided Design 2011; 43(1) :67-71.
[14] Li G, Sun J, Li J. Modeling and analysis of helical groove grinding in end mill machining. J Mater Process Tech 2014; 214(12):3067-3076.
[15] Chiang CJ, Fong ZH. Undercutting and interference for thread form grinding with a tilt angle. Mech Mach Theory 2009; 44(11):2066-2078.
[16] Chiang CJ, Fong ZH, Tseng JT. Computerized simulation of thread form grinding process. Mech Mach Theory 2009; 44(4):685-696.
[17] Bar G. CAD of worms and their machining tools. Comput Graph-UK 1990; 14(3-4):405-411.
[18] Mohan LV, Shunmugam MS, Simulation of whirling process and tool profiling for machining of worms. J Mater Process Tech 2007; 185(1-3):191-197.
[19] Oancea N, Popa I, Teodor VG, Oancea VG. Tool profiling for generation of discrete helical surfaces. Int J Adv Manuf Tech 2010; 50(1-4):37-46.
[20] Fromentin G, Poulachon G. Modeling of interferences during thread milling operation. Int J Adv Manuf Tech 2010; 49(1):41-51.
[21] Fromentin G, Poulachon G, Moisan A, Julien B, Giessler J. Precision and Surface Integrity of Threads Obtained by Form Tapping. CIRP Ann-Manuf Techn. 2005; 54(1):519-522.